Send Orders for Reprints to reprints@benthamscience.net

Current Molecular Medicine, **XXXX,** ***XX,*** **1-14**

RESEARCH ARTICLE

Neuroprotective Potential of Conditioned Medium from Adipose and Liver Mesenchymal Stem Cells in a Rat Model of Global Cerebral Ischemia-Reperfusion Injury

Maryam Khombi Shooshtari[1,2,#], Sadegh Moradi Vastegani[2,#], Yaghoob Farbood[2], Alireza Sarkaki[2], Vahid Bayati[3], Fereshteh Nejaddehbashi[3], Seyed Esmaeil Khoshnam[2,*], Maryam Farzaneh[4,5,*]

[1]Chronic Renal Failure Research Center, Ahvaz Jundishapur University of Medical Sciences, Ahvaz, Iran; [2]Persian Gulf Physiology Research Center, Medical Basic Sciences Research Institute, Ahvaz Jundishapur University of Medical Sciences, Ahvaz, Iran; [3]Cellular and Molecular Research Center, Medical Basic Sciences Research Institute, Ahvaz Jundishapur University of Medical Sciences, Ahvaz, Iran; [4]Fertility, Infertility and Perinatology Research Center, Ahvaz Jundishapur University of Medical Sciences, Ahvaz, Iran; [5]Clinical Research Development Unit, Imam Khomeini Hospital, Ahvaz Jundishapur University of Medical Sciences, Ahvaz, Iran

ARTICLE HISTORY

Received: September 05, 2024
Revised: January 19, 2025
Accepted: January 31, 2025

DOI:
10.2174/0115665240351634250506164609

Abstract: ***Background*****:** Mesenchymal stem cell-derived conditioned medium (MSC-CM) contains bioactive factors that provide neuroprotection in cases of cerebral ischemia-reperfusion (IR) injury. This study aimed to compare the therapeutic potential of rat adipose-derived MSC-CM (rAD-MSC-CM) and chicken embryo liver-derived MSC-CM (cLD-MSC-CM) following global cerebral IR injury in male rats.

Material and Methods**:** We harvested rAD-MSC-CM from the adipose tissue surrounding the epididymis of Wistar rats and cLD-MSC-CM from the liver tissue of 10-day-old chicken embryos. To induce global cerebral ischemia, we utilized a four-vessel occlusion (4VO) model in rats. After inducing ischemia, the conditioned media were administered via intravenous injection 30 minutes post-reperfusion. We evaluated the cognitive and non-cognitive functions of the animals using standard behavioral tests. Additionally, we assessed blood-brain barrier (BBB) permeability, brain water content (BWC), oxidative-antioxidative status, and conducted histopathological analyses of the hippocampal tissue in the IR rats.

Results**:** Our findings demonstrated that treatment with both rAD-MSC-CM and cLD-MSC-CM significantly improved memory function, reduced anxiety- and depression-like behaviors, and enhanced exploratory activities. These behavioral improvements correlated with decreased BBB permeability and BWC, reduced oxidative stress, and mitigated histopathological changes in the hippocampal tissue.

Conclusion**:** Our findings suggest that both rAD-MSC-CM and cLD-MSC-CM offer protective benefits against IR injury, likely owing to their antioxidant properties.

Keywords: Mesenchymal stem cells, Adipose, Liver, Conditioned medium, Chicken embryo, Ischemic stroke, Rat.

1. INTRODUCTION

Stroke is a severe acute cerebrovascular disease that results in high mortality rates and long-term physical disabilities for individuals worldwide [1]. Ischemic stroke, which accounts for over 85% of all acute strokes, is caused by the blockage of cerebral arteries and is more prevalent among older individuals [2]. The pathophysiological consequences of stroke can lead to neuronal cell death and brain damage [3]. Current therapeutic approaches are limited to tissue plasminogen activator (tPA)-induced reperfusion and mechanical thrombectomy [4]. However, the narrow therapeutic window of tPA therapy highlights the urgent need for new neuroprotective strategies for ischemic stroke patients [3].

Numerous studies have shown that transplanted mesenchymal stem cells (MSCs) can decrease infarct volume and enhance functional recovery in animal models of ischemic stroke [5, 6]. It is now understood

*Address correspondence to these authors at the Persian Gulf Physiology Research Center, Medical Basic Sciences Research Institute, Ahvaz Jundishapur University of Medical Sciences, Ahvaz, Iran; Tel: +989171491729; Fax: +986133738248;
E-mail: Esmaeil.khoshnam1392@gmail.com
Fertility, Infertility and Perinatology Research Center, Ahvaz Jundishapur University of Medical Sciences, Ahvaz, Iran;
E-mail: Maryamfarzaneh2013@yahoo.com
[#]*These authors contributed equally to this work.*

that transplanted MSCs primarily create an environment conducive to tissue repair rather than serving as a direct cell replacement therapy [7]. This process likely involves the release of growth factors, cytokines, chemokines, neurotrophins, and extracellular vesicles, collectively known as the secretome [8, 9]. Extensive evidence indicates that the MSCs-secretome has a positive effect on cerebral ischemic injury [10]. It accomplishes this by lowering oxidative stress through the inhibition of reactive oxygen species (ROS) and reactive nitrogen species (RNS) production, as well as by transferring healthy mitochondria to damaged cells [9].

The degree of neuronal loss and synaptic disruption in this area can serve as a predictor for the severity of cognitive dysfunction following a stroke [11]. The histopathological changes identified in the CA1 region are closely linked to cognitive impairments, including memory deficits [12].

Recently, stem cell therapy has emerged as a promising new option for treating ischemic stroke [13]. However, implementing stem cell transplantation in clinical practice presents several challenges. The procedures involved are often complex and invasive, requiring a high level of expertise [14]. Moreover, there are risks associated with this therapy, including the potential for tumor formation, a considerable chance of the body rejecting the transplanted cells, and low survival rates for those cells after transplantation [15]. To tackle these issues, the use of "cell-free therapeutics," like conditioned medium (CM), offers a promising alternative to traditional cell-based treatments [16, 17]. Recent studies have shown that MSCs-CM contains a variety of bioactive molecules that could improve outcomes in animal models of ischemia-reperfusion (IR) [18, 19]. As a result, administering MSC-CM has been shown to enhance recovery in rodent models of cerebral ischemia [20-22]. The clinical application of these acellular approaches, which avoid using cells, is generating considerable interest as potential regenerative therapies [23]. They sidestep the risks of immune rejection and tumor formation that are associated with cell transplantation [24]. Previous studies have discovered that cell-free extract derived from adipose stem cells exhibits neuroprotective effects in experimental stroke models [25]. Additionally, this extract has been shown to reduce brain atrophy volume and improve both neuromotor and cognitive functions in a mouse model of ischemic stroke [26].

So far, the effects of chicken embryo liver-derived MSC-CM (cLD-MSC-CM) have not been evaluated on global cerebral IR injury. Here, we compared the functional roles of cLD-MSC-CM to those of rat adipose-derived MSC-CM (rAD-MSC-CM) in the IR injury model. Consequently, we aimed to determine whether systemic treatment with rAD-MSC-CM and cLD-MSC-CM enhances recovery following global cerebral IR injury in male rats.

2. MATERIALS AND METHODS

2.1. Animals

Adult male Wistar rats weighing between 200 and 250 grams, aged 7–8 weeks, were housed in standard cages under controlled conditions, with a temperature of 22 ± 2°C and humidity levels of 55–60%. Rats were sourced from the AJUMS animal house. They were kept on a 12-hour light/dark cycle and had unlimited access to standard food and tap water. All experimental procedures followed NIH guidelines and were permitted by the ethics committee at AJUMS (Ethic code: IR.AJUMS.ABHC.REC.1400.075).

2.2. Preparation of rAD-MSC-CM

MSCs were isolated from the adipose tissues surrounding the epididymis of the male rats [27]. The tissue samples were gently minced into small tubes and incubated with a 0.1% solution of collagenase type I (15 minutes, 37°C). After digestion, the mixture was diluted with 4 ml of DMEM medium (Dulbecco's Modified Eagle's Medium) (Gibco, USA) supplemented with 15% FBS (fetal bovine serum) (Gibco, USA) and centrifuged at 1500 rpm for 15 minutes to separate the MSC pellet from adipocytes. The supernatant was discarded, and the cellular pellet was filtered through a nylon mesh (200 µm pore size) to remove any undigested tissue fragments. An aliquoted cell suspension was seeded into culture dishes containing DMEM-High Glucose supplemented with 15% FBS, 100 U/ml penicillin, and 100 µg/ml streptomycin. The cultures were maintained at 37°C in a humidified atmosphere with 5% CO_2. After approximately 48 hours, the first medium change was completed, and non-adherent cells were eliminated. The medium was changed every 2 to 3 days. When the MSCs reached 80–90% confluence, they were incubated with 0.05% trypsin (Sigma, USA) and 0.02% ethylenediaminetetra-acetic acid (EDTA) for passage.

MSCs from passage 2 were incubated in serum-free culture medium to prepare conditioned medium. After two passages, when the MSCs reached a density of 3 to 4 × 10^5 cells/ml, they were incubated in serum-free culture medium to prepare CM. After five days, the MSC-derived conditioned medium was collected. MSCs-derived supernatants were then centrifuged and filtered to eliminate any debris. The protein concentration of rAD-MSC-CM was measured using a protein assay kit (Thermo Fisher Scientific, Pierce™ BCA), resulting in a concentration range of 800-1200 µg/ml.

2.3. Preparation of cLD-MSC-CM

MSCs were isolated from the liver tissue of a chicken embryo [28, 29]. Five embryonated chicken eggs at stage X were incubated at 37.5°C with 60-65% humidity for 10 days until they reached stage HH35. After the incubation period, the embryos were separated from the yolk and extraembryonic tissues. The liver tissue was aseptically dissected and

transferred to a sterile petri dish containing phosphate-buffered saline (PBS). The liver tissue was cut into small pieces and placed in a sterile tube with Trypsin-EDTA enzyme solution (0.25% Trypsin and 2.25 mM EDTA) for 10 minutes. Following digestion, the enzyme was inactivated by adding DMEM with 10% FBS. The cell suspension was then centrifuged at 1200 rpm for 5 minutes. The cell pellet was resuspended and transferred to gelatin (0.1%) coated culture plates containing DMEM/F12 with 10% FBS medium. The plates were incubated at 37°C in a 5% CO_2 atmosphere. After two days of incubation, the growth and proliferation of hepatocytes were observed using an inverted microscope. When the MSCs reached 80–90% confluence, they were incubated with 0.05% trypsin for passaging. After two passages, when the MSCs reached a density of 3 to 4 × 10^5 cells/ml, they were incubated in serum-free culture medium to prepare CM. Due to the rapid proliferative rates of cLD-MSCs, the MSC-CM was collected after three days. MSCs- CM were then centrifuged and filtered to remove any debris. The protein concentration of cLD-MSC-CM was measured, yielding a concentration range of 800-1200 µg/ml.

2.4. Induction of Global Cerebral Ischemia

The four-vessel occlusion (4VO) model was employed to induce global cerebral IR as described by Sun et al. [30]. Following induction of anesthesia using ketamine and xylazine (Alfasan Chemical Co., Netherlands) (100/10 mg/kg), and placement of the rats in a stereotaxic device, the posterior area of the neck was disinfected using 5% Betadine. A midline incision was made through the skin and muscles along the posterior neck. The two vertebral arteries, located beneath the alar foramen of the first cervical vertebra, were cauterized using electrocoagulation to achieve permanent occlusion. The incision was then sutured. After the initial recovery, the rats were returned to their cages. The following day, the rats were anesthetized again and placed in a supine position. A scalpel incision was made along the anterior neck, and the fascia and muscles were carefully dissected to expose the carotid arteries. The carotid arteries and vagus nerves were separated, and both common carotid arteries were simultaneously occluded using microvascular clamps for 20 minutes to induce the ischemic phase. After the ischemic period, micro-clamps were released to restore blood flow, marking the onset of the reperfusion phase. The confirmation of IR was assessed by observing the disappearance of dilated pupils and the absence of the corneal reflex. Throughout the surgical procedure, the rats' body temperature was monitored and maintained at 37°C using a heating blanket. After complete recovery, the rats were returned to their cages once again.

2.5. Experimental Groups

A total of 68 rats, excluding those who died after induction of 4VO model, were randomly assigned to four experimental groups:

a) Control group: Received basic culture medium (DMEM/F12) (500 µl/each rat, i.v.) 30 minutes after 4VO surgery without artery occlusion.

b) IR group: Received basic culture medium (DMEM/F12) (500 µl/each rat, i.v.) 30 minutes after induction of 4VO model.

c) IR+rAD-MSC-CM group: Received a single injection of rAD-MSC-CM (500 µl/each rat, i.v.) 30 minutes after induction of 4VO model.

d) IR+cLD-MSC-CM group: Received a single injection of cLD-MSC-CM (500 µl/each rat, i.v.) 30 minutes after induction of 4VO model.

A schematic diagram of the experimental procedure has been provided in Fig. (**1**).

2.6. Passive Avoidance Test (PAT)

The study evaluated passive avoidance learning and memory functions using a shuttle box apparatus. The apparatus consisted of two interconnected chambers, one light and one dark, separated by a door. The chambers' floors consisted of stainless-steel rods that could be electrified in the dark using a shock generator (Borj Sanat Co., Tehran-Iran). The experiment was conducted in two adaptation and training phases. In the adaptation phase, animals were allowed to familiarize themselves with the apparatus. In the training phase, the animal was located in the lighted compartment, and the door was opened. The entrance latency into the dark compartment was considered as the IL (initial latency). Upon entering the dark compartment, the door was instantly closed, and an electrical shock was initiated (1 mA, 50 Hz, 3 seconds). This practice was repeated every 5 minutes until the animal stayed constantly in the light compartment for 120 seconds. Finally, 24 hours after the training phase, the retention phase was done, in which the step-through latency (STL) was recorded. In this test, memory performance shows a positive correlation with STL, which is regarded as memory consolidation. No shock was administered during the retention phase, and a maximum cutoff time of 300 seconds was established.

2.7. Elevated Plus Maze Test (EPM)

This apparatus was utilized to assess anxiety-like behaviors in rats. The EPM consists of open and closed arms that cross with a central square and are elevated 50 cm above the ground. During the test, rats were positioned in the central square, and their behavior was videoed for 5 minutes. The recorded data were analyzed using Maze Router software (V3.1, Techniq Azma Co, Tabriz-Iran). Two key metrics were considered as anxiety-like behaviors:

1) Open Arm Entry (%OAE): Calculated as the number of entries into the open arms divided by the total entries into both open and closed arms, multiplied by 100.

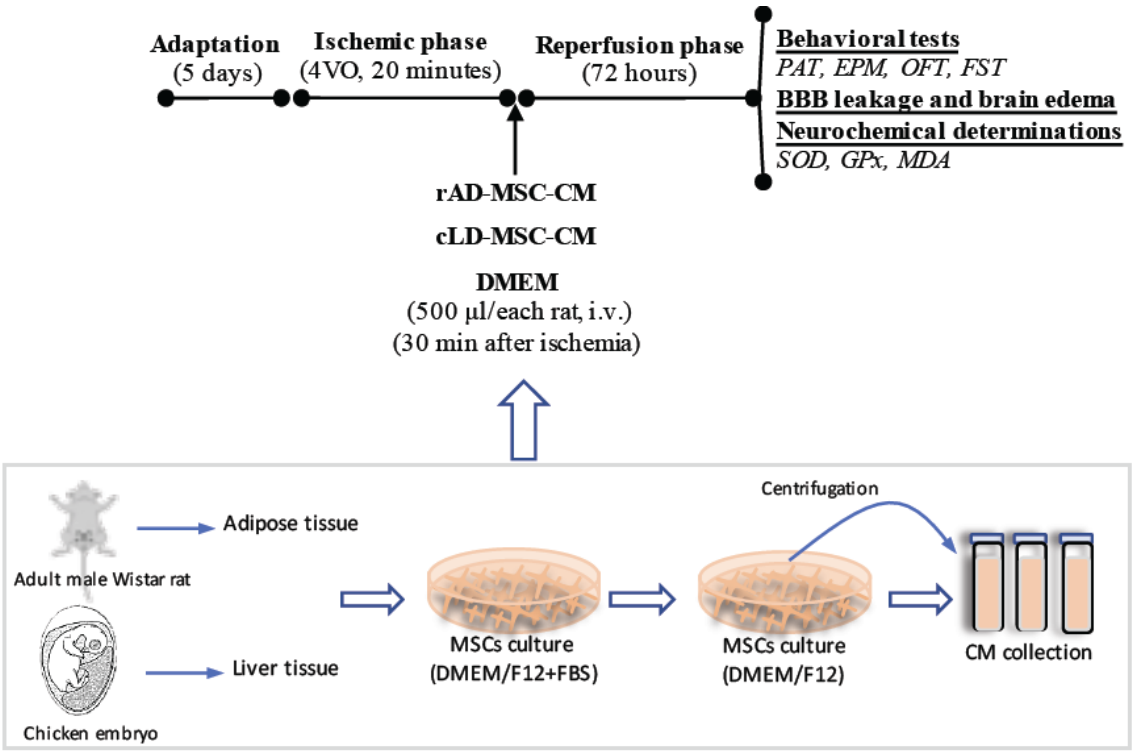

Fig. (1). Schematic timeline of experimental design. 4VO: four-vessel occlusion; MSC: mesenchymal stem cell; CM: conditioned medium; rAD-MSC-CM; rat adipose-derived MSC-CM; cLD-MSC-CM: chicken embryo liver-derived MSC-CM; EPM: elevated plus maze; OFT: open field test; FST: forced swimming test; BBB: blood brain barrier; MDA: malondialdehyde; GP_X: glutathione peroxidase; SOD: superoxide dismutase. (*A higher resolution / colour version of this figure is available in the electronic copy of the article*).

2) Open Arm Time (%OAT): Determined as the time spent in the open arms divided by the total time spent in all arms, multiplied by 100.

2.8. Forced Swimming Test (FST)

In this study, we employed the FST to assess depressive-like behavior in rats. The FST involved placing each rat in a Plexiglas cylinder filled with water (20 cm in diameter and 50 cm in height). Following a 1-minute habituation period, the immobility and straggling time of the rats were recorded over a subsequent 5-minute observation period. In this context, increased immobility and decreased straggling were interpreted as a reduction in the animal's motivation to escape, which serves as an indicator of depressive-like behavior.

2.9. Open Field Test (OFT)

For the OFT, the apparatus consisted of a box measuring 50 × 50 × 50 cm, divided into 25 equal squares. Each animal was placed individually at the box's center, and their behavior was videoed for 5 minutes. The recorded data were subsequently analyzed using a specified software (Maze Router, V3.1, Techniq Azma Co, Tabriz-Iran). During the test, we evaluated several behaviors, including exploration (indicated by rearing) and anxiety (assessed through grooming behavior).

2.10. Determination of Blood-Brain Barrier (BBB) Permeability

To evaluate the permeability of the BBB, we employed Evans blue infiltration into brain tissue [31]. The procedure was carried out as follows: Anesthetized rats received an intravenous injection of Evans blue (20 mg/kg in 1 ml of saline) through the tail veins. After one hour, the rats underwent intracardiac perfusion with 200–300 mL of saline to eliminate any intravascular Evans blue. After perfusion, the brain was harvested from the skull and homogenized in 1 ml of TCA (trichloroacetic acid). The homogenate was incubated in a 4°C freezer for 2–3 minutes, centrifuged at 2000 g for 10 minutes, and diluted in ethanol at a ratio of 3:1. The absorbance of the resulting solution was measured at 620 nm using a spectrophotometer. The concentration of Evans blue was determined based on a linear standard curve and presented as micrograms of Evans blue per milliliter (µg/ml) [32]. An increase in Evans blue concentration indicated enhanced brain vessel permeability, suggesting a disruption in the BBB integrity [33].

2.11. Brain Water Content (BWC)

To assess brain edema after IR, we measured the water content of brain tissue. Brain samples were carefully collected from the skulls of rats that were under deep anesthesia. Using a digital scale, we

recorded the wet weight (WW) of the brain tissue as described by Gerriets *et al*. [34]. The tissue samples were then placed in an oven set to 110 °C for 24 hours to determine the dry weight (DW). Finally, we calculated the percentage of BWC by the subsequent formula: BWC =(WW−DWWW) ×100BWC = (WWWW−DW)×100

2.12. Collection of the ELISA Samples

Following induction of deep anesthetization, the brain samples were precisely extracted, and the hippocampal samples were quickly excised on an ice-cold plate, quietly rinsed with cold saline, and then stored ina freezer (-80°C) until further evaluation. The samples were homogenized in a cold buffer specifically designed for homogenization, which contained PBS and a protease inhibitor cocktail from Roche Co., Switzerland. The homogenates were centrifuged at 10,000 ×g for 20 minutes at 4°C. The supernatants were then aliquoted and reserved for subsequent ELISA assays.

2.13. Assessment of Oxidative Indices

To assess oxidative stress in the hippocampal samples, we measured the activities of superoxide dismutase (SOD) and glutathione peroxidase (GPX) enzymes (ZELL bio-Co., Germany) and the concentration of malondialdehyde (MDA) (ZELL bio-Co., Germany) following the protocols provided by the manufacturers. The SOD and GPX enzyme activities were expressed as U per mg of protein, and the MDA levels were reported as nmol per mg of protein.

2.14. Histopathological assessment

The animals were subjected to deep and irreversible anesthesia through an overdose of a ketamine/xylazine mixture (100/10 mg/kg). Following this procedure, brain samples were meticulously extracted for histopathological analysis and subsequently fixed in a 10% buffered formalin solution. The samples were then embedded in paraffin, and serial sections of 5 µm thickness were prepared from the targeted regions using a microtome. These sections were stained with hematoxylin and eosin (H&E), allowing for a thorough examination of histopathological changes under a light microscope [31].

2.15. Statistical Analysis

The results were expressed as mean ± standard error of the mean (SEM). The Kolmogorov–Smirnov test was used to confirm the normal distribution of the data. Parametric one-way analysis of variance (ANOVA) followed by Tukey's post hoc test was employed for data analysis. Statistical analyses were performed using GraphPad Prism 6 software (GraphPad Software Inc., San Diego, USA). A p-value less than 0.05 ($p < 0.05$) was considered statistically significant.

3. RESULTS

3.1. PAT

Current findings indicated that STL was meaningly reduced in the IR group in comparison to the control group ($F (3, 24) = 35.37$; $p < 0.001$, Fig. **2**). However, administration of MSCs-derived CM in the rAD-MSC-CM and cLD-MSC-CM groups resulted in a marked increase in STL compared to the IR group ($p < 0.001$ for both treatments).

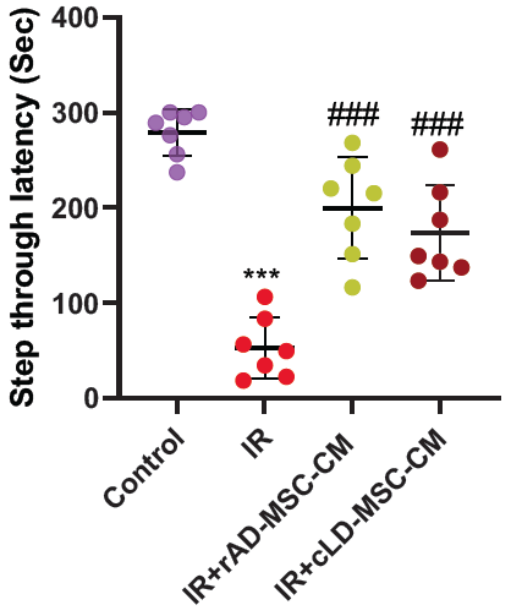

Fig. (2). Effects of rAD-MSC-CM (500 µl/each rat, i.v.) and cLD-MSC-CM (500 µl/each rat, i.v.) on step-through latency in the PAT following IR induction using a 4VO model in male rats. 4VO: four-vessel occlusion; IR: ischemia reperfusion; MSC: mesenchymal stem cell; CM: conditioned medium; rAD-MSC-CM; rat adipose-derived MSC-CM; cLD-MSC-CM: chicken embryo liver-derived MSC-CM. Data were demonstrated as mean ± SD (n = 7). ***$p < 0.001$ vs. control group, ###$p < 0.001$ *vs*. IR group (one-way ANOVA). (*A higher resolution / colour version of this figure is available in the electronic copy of the article*).

3.2. FST

Immobility and struggling times were measured in the FST to assess depressive-like behavior. The results showed a significant increase in immobility time in the "IR" group compared to the control group ($F (3, 24) = 20.95$; $p < 0.001$, Fig. **3A**). In contrast, immobility time was significantly reduced in the rAD-MSC-CM and cLD-MSC-CM groups compared to the IR group ($p < 0.001$ for both treatments).

The results demonstrate a significant decrease in struggling time in the "IR" group compared to the control group ($F (3, 24) = 16.33$; $p < 0.001$, Fig. **3B**). In contrast, immobility time was significantly elevated in the rAD-MSC-CM and cLD-MSC-CM groups compared to the IR group ($p < 0.001$ and $p < 0.05$, respectively).

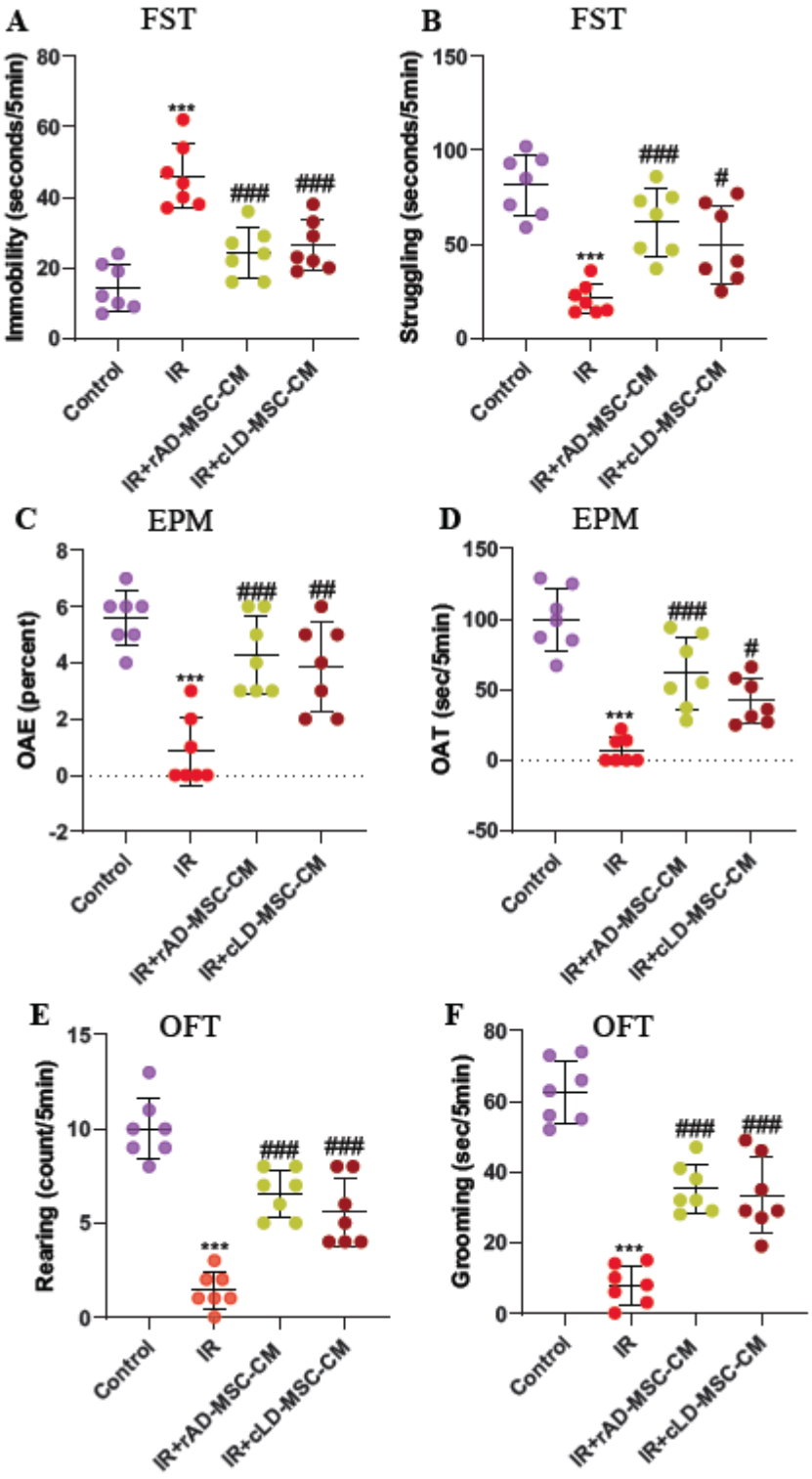

Fig. (3). Effects of rAD-MSC-CM (500 µl/each rat, i.v.) and cLD-MSC-CM (500 µl/each rat, i.v.) on depressive like behaviors, anxiety like behaviors, exploratory activities IR rats (using 4VO model) were represented using FST, EPM and OFT, respectively. (Panel **A** and **B**) represents duration of immobility and struggling in FST. (Panel **C** and **D**) represents OAE and OAT in EPM. (Panel **E** and **F**) indicates rearing (exploratory) and grooming (anxiety like behavior) activities in OFT. 4VO: four-vessel occlusion; IR: ischemia-reperfusion; MSC: mesenchymal stem cell; CM: conditioned medium; rAD-MSC-CM; rat adipose-derived MSC-CM; cLD-MSC-CM: chicken embryo liver-derived MSC-CM. FST: forced swimming test; EPM: elevated plus maze; OFT: open field test; OAE: open arm entries; OAT: open arm time. Data were demonstrated as mean ± SD (n = 7). ***p < 0.001 vs. control group, ###p < 0.001, ##p < 0.01 and #p < 0.05 vs. IR group (one-way ANOVA). (*A higher resolution / colour version of this figure is available in the electronic copy of the article*).

3.3. EPM

To assess anxiety-related behaviors, the OAE (open arm entry) and OAT (open arm time) parameters were measured in the EPM test. These parameters were found to be significantly decreased in the IR group compared to the control group (OAE: F (3, 24) = 16.36; OAT: F (3, 24) = 27.75; $p < 0.001$ for both parameters, see Fig. **3C** and **3D**). Conversely, treatment with rAD-MSC-CM and cLD-MSC-CM markedly increased both OAE ($p < 0.001$ and $p < 0.01$, respectively) and OAT ($p < 0.001$ and $p < 0.05$, respectively) compared to the IR group.

3.4. OFT

Rearing activity, which serves as an indicator of exploratory behavior, was significantly lower in the IR group in comparison to the control group (F (3, 24) = 40.91; $p < 0.001$, Fig. **3E**). In contrast, both the rAD-MSC-CM and cLD-MSC-CM groups showed a significant increase in rearing when compared to the IR group ($p < 0.001$ for both treatments).

Grooming activity in the OFT was assessed as an indicator of anxiety-related behavior. The results showed a significant decrease in grooming in the IR group compared to the "control" group (F (3, 24) = 51.56; $p < 0.001$, see Fig. **3F**). Additionally, grooming behavior was significantly increased in both rAD-MSC-CM and cLD-MSC-CM groups compared to the IR group ($p < 0.001$ for both treatments).

3.5. BBB Permeability and Brain Water Content

The concentration of Evans blue in brain samples was evaluated to assess leakage of the BBB in the IR rats. The results revealed that Evans blue concentration was significantly elevated in the IR group in comparison to the control group (F (3, 16) = 44.26; $p < 0.001$, see Fig. **4A**). In contrast, EB concentration was markedly reduced in the rAD-MSC-CM and cLD-MSC-CM groups compared to the IR group ($p < 0.001$ for both treatments).

The percentage of BWC serves as an indicator of edema in brain tissue, which was significantly higher in the IR group in comparison to the control group (F (3, 16) = 26.70; $p < 0.001$, see Fig. **4B**). However, BWC was significantly reduced in the rAD-MSC-CM and cLD-MSC-CM groups compared to the IR group ($p < 0.001$ and $p < 0.01$, respectively).

3.6. Oxidative Stress Indices

The SOD and GPx enzyme activities were evaluated to assess antioxidant function in the hippocampal samples of IR rats. Current findings indicate that SOD and GPx activities were significantly reduced in the IR group of the hippocampus compared to the control group (F (3, 20) = 10.52 and F (3, 20) = 10.76, respectively; $p < 0.001$ for both enzymes, Fig. **5A** and **5B**). In contrast, the SOD and GPx enzyme activities were markedly increased in the rAD-MSC-CM and cLD-MSC-CM groups compared to the IR group ($p < 0.01$ and $p < 0.05$ for both enzymes, respectively). Additionally, we evaluated the concentration of MDA in the hippocampal tissue, which showed that IR injury significantly elevated MDA levels in the IR group in comparison to the control group (F (3, 20) = 19.78; $p < 0.001$, see Fig. **5C**). Conversely, MDA concentration was significantly decreased in the rAD-MSC-CM and cLD-MSC-CM groups compared to the IR group ($p < 0.01$ for both treatments).

3.7. Histopathology

The histological analyses were performed to evaluate the histopathological changes in the CA1 region of hippocampal samples. In the control group,

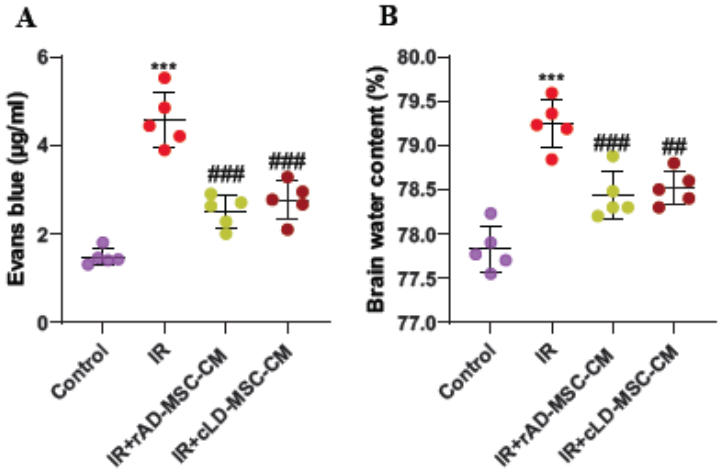

Fig. (4). Effects of rAD-MSC-CM (500 µl/each rat, i.v.) and cLD-MSC-CM (500 µl/each rat, i.v.) on BBB permeability (**A**) and brain edema (**B**) were demonstrated in Evans blue test dusty following IR induction using a 4VO model in male rats. BBB: blood brain barrier; 4VO: four-vessel occlusion; IR: ischemia-reperfusion; MSC: mesenchymal stem cell; CM: conditioned medium; rAD-MSC-CM; rat adipose-derived MSC-CM; cLD-MSC-CM: chicken embryo liver-derived MSC-CM. Data were demonstrated as mean ± SD (n = 5). ***$p < 0.001$ *vs*. control group, ###$p < 0.001$ and ##$p < 0.01$ *vs*. IR group (one-way ANOVA). (*A higher resolution / colour version of this figure is available in the electronic copy of the article*).

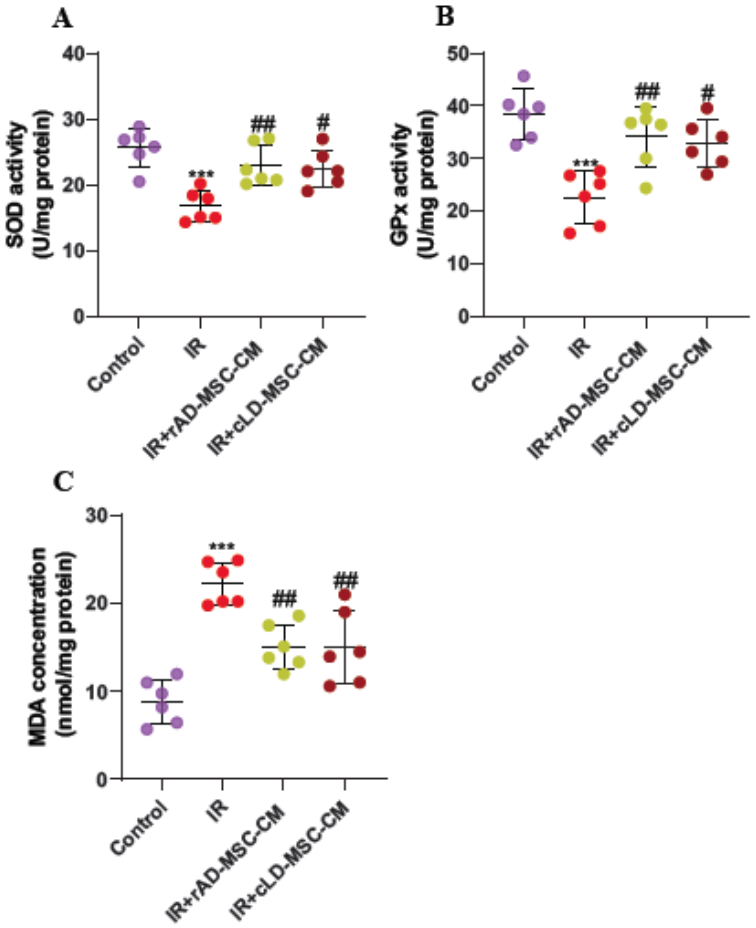

Fig. (5). Effects of rAD-MSC-CM (500 µl/each rat, i.v.) and cLD-MSC-CM (500 µl/each rat, i.v.) on oxidative status namely SOD activity (**A**), GPx activity (**B**), and tissue level of MDA (**C**) in the hippocampal tissues using ELISA assays following IR induction in male rats. MDA: malondialdehyde; GP_X: glutathione peroxidase; SOD: superoxide dismutase; IR: ischemia-reperfusion; MSC: mesenchymal stem cell; CM: conditioned medium; rAD-MSC-CM; rat adipose-derived MSC-CM; cLD-MSC-CM: chicken embryo liver-derived MSC-CM. Data were demonstrated as mean ± SD (n = 6). ***p < 0.001 vs. control group, ##p < 0.01 and #p < 0.05 vs. IR group (one-way ANOVA). (*A higher resolution / colour version of this figure is available in the electronic copy of the article*).

the pyramidal cell layer (PCL) showed closely packed cell bodies of pyramidal neurons with vesicular nuclei, while the polymorphic layer (POL) and molecular layer (ML) exhibited glial cells alongside normal blood capillaries (Fig. **6A** and **6B**). In contrast, the IR group displayed significant alterations in the CA1 region, characterized by status spongiosis. The pyramidal cell bodies in the PCL were shrunken and exhibited pyknotic nuclei. Additionally, both the POL and ML showed an increase in the number of blood capillaries, along with dilation and edema in the Virchow-Robin spaces surrounding these capillaries, accompanied by neurogliosis and intracellular edema in interstitial neurons (Fig. **6C** and **6D**). In the rAD-MSC-CM group, the CA1 region revealed a few shrunken pyramidal cell bodies with pyknotic nuclei in the PCL. The POL and ML also exhibited dilation and edema in the Virchow-Robin spaces around blood capillaries (Fig. **6E** and **6F**). Similarly, in the cLD-MSC-CM group, there were a limited number of shrunken pyramidal cell bodies with pyknotic nuclei in the PCL, while the POL and ML displayed dilated blood capillaries (Fig. **6G** and **6H**).

4. DISCUSSION

In the present study, we demonstrated that the 4VO model of cerebral IR injury led to memory damage, anxiety, and depressive-like behaviors, and reduced exploratory activities in male rats. These behavioral changes were attended by increased BBB leakage and brain edema. Furthermore, we found that these functional deficits were associated with elevated oxidative stress markers in the hippocampal tissue of experimental animals. We are the first to compare the effects of rAD-MSC-CM and cLD-MSC-CM in the treatment of IR injury. Our findings provide experimental evidence that administering CM can help reduce brain injury in a 4VO rat model. Furthermore, our data indicates that the reduction of BBB infiltration and oxidative stress markers may play a significant role

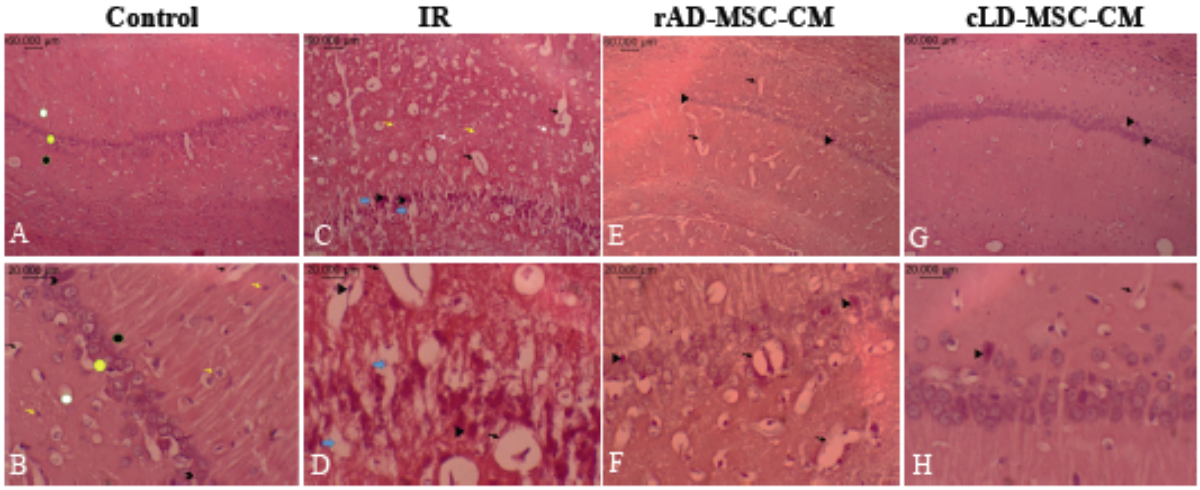

Fig. (6). Effects of rAD-MSC-CM (500 µl/each rat, i.v.) and cLD-MSC-CM (500 µl/each rat, i.v.) on histopathology changes in the CA1 area were presented in different experimental groups. Control (**A** and **B**), IR (**C** and **D**), rAD-MSC-CM (**E** and **F**), cLD-MSC-CM (**G** and **H**). White circle: Polymorphic layer; yellow circle: pyramidal cell layer; black circle: molecular layer; arrowhead shrunken and pyknotic pyramidal cell bodies; yellow arrow: neurogliosis; black arrow: dilated blood capillaries; blue arrow: spongiosis status; white arrow: intracellular edema in interstitial neurons; IR: ischemia-reperfusion; MSC: mesenchymal stem cell; CM: conditioned medium; rAD-MSC-CM; rat adipose-derived MSC-CM; cLD-MSC-CM: chicken embryo liver-derived MSC-CM. (*A higher resolution / colour version of this figure is available in the electronic copy of the article*).

in the positive effects seen with both rAD-MSC-CM and cLD-MSC-CM.

rAD-MSC and cLD-MSC offer several advantages over other sources of stem cells, particularly from a clinical perspective. rAd-MSCs are abundant and easily accessible, allowing for their isolation through minimally invasive procedures, which makes them ideal for both research and therapeutic applications [35, 36]. Their immunomodulatory properties enhance their effectiveness in regenerative medicine [37]. Adipose MSCs exhibit superior proliferative capacity and stronger immunosuppressive properties, making them less likely to provoke immune rejection when used in autologous transplants [38, 39]. Besides, chicken embryo-liver MSCs present unique developmental features that could provide valuable insights into cellular behavior and differentiation [40, 41]. Additionally, using rat adipose tissue and chicken embryos raises fewer ethical concerns compared to human tissues or embryonic stem cells. By leveraging the properties of rAD-MSC and cLD-MSC, researchers can explore innovative therapeutic strategies for various diseases, particularly those associated with tissue damage and degeneration. Overall, these sources not only facilitate easier access and isolation but also offer promising avenues for advancing regenerative medicine.

Cognitive impairment and memory loss frequently occur following ischemic stroke, with approximately one-third of patients showing signs of dementia within a year [42]. In this study, the induction of IR injury led to impaired performance in rats during the PAT, a measure used to evaluate cognitive impairment. In this experiment, the rats learned to associate entry into a dark chamber with an electrical shock, and their ability to avoid this compartment was interpreted as an indicator of cognitive function [43]. Our findings revealed that IR injury significantly reduced the STL, indicating a decline in cognitive abilities among the animals. These results are consistent with previous studies that demonstrated significant cognitive and memory decline in animal models following ischemic stroke [44, 45]. After cerebral ischemia, several changes, including delayed neuronal death in the CA1 region of the hippocampus [46], decreased activity in the prefrontal cortex, and thinning of the entorhinal cortex have been observed [47]. These changes in brain structure and function, especially in areas critical for memory processing like the hippocampus and prefrontal cortex, can result in significant memory deficits following ischemic stroke [48, 49]. While numerous studies have explored the positive effects of neuroprotectants, there has been limited research focusing on the long-term impact of these compounds or interventions on cognitive impairment. Notably, the learning and memory indices related to the PAT showed significant improvement in rats treated with rAD-MSC-CM and cLD-MSC-CM. This enhancement indicates the protective effects of these treatments against cognitive impairments induced by IR injury. The neuroprotective effects of MSCs in stroke management are increasingly attributed to their secretion of a diverse array of bioactive molecules, which exert their influence in an autocrine or paracrine fashion [50]. MSCs demonstrate remarkable therapeutic plasticity, enabling them to adjust their fate and functions in response to pathological conditions, thereby enhancing brain repair processes [51, 52]. Consequently, utilizing MSCs-CM presents a promising strategy for the treatment of ischemic stroke [53].

Research has consistently demonstrated that ischemic stroke is associated with symptoms of depression and anxiety in patients [54, 55]. It is hypothesized that these psychological effects may be induced by the stroke itself [56]. In animal studies, rats with induced ischemia displayed increased anxiety- and depression-like behaviors in tests such as EPM and FST [54, 57], which aligns with our findings. Specifically, the OAT and OAE in the EPM indicate anxiety-like behaviors in IR rats. Furthermore, the immobility time measured in the FST, which is associated with depressive behavior, was also found to be elevated following IR induction. Our key finding is that MSC-CM has been shown to alleviate anxiety- and depression-like behaviors in IR rats, likely due to its anxiolytic and antidepressant properties [58]. Moreover, our results demonstrated that rearing (as exploratory behavior) and grooming (as anxiety behavior) in the open field apparatus were significantly reduced in the ischemic rats. These findings are consistent with those reported in other studies [59, 60]. However, treatment with rAD-MSC-CM and cLD-MSC-CM alleviated these behavioral deficits in rats challenged by cerebral ischemia. The beneficial effects of MSC-CM have been documented in animal models as well, which is attributed to its ability to modulate oxidative stress and neuroinflammation in various brain regions [61, 62].

The current study demonstrated that Evans blue leakage into the brain was significantly increased in the 4VO ischemic models, indicating heightened BBB permeability. This aligns with findings from other studies that have also reported increased BBB permeability in rats with cerebral ischemia [63]. Growing evidence suggests that the production of ROS plays a critical role in disrupting the BBB by breaking down tight junction proteins [64].

MSC-CM contains a variety of antioxidant proteins that play roles in regulating apoptosis and promoting cell proliferation [65]. This indicates that MSC-CM has inherent antioxidant properties that may enhance its therapeutic potential. In this context, it is suggested that rAD-MSC-CM and cLD-MSC-CM reduce BBB permeability, likely due to these antioxidant properties.

It has also been shown that cerebral IR injury can cause cerebral edema in ischemic rats [66], which aligns with our findings. This cerebral edema resulting from ischemic stroke can lead to a range of clinical complications, including behavioral and cognitive impairments, memory loss, and mental dysfunctions [67]. Therefore, treatment with rAD-MSC-CM and cLD-MSC-CM may help alleviate the effects of cerebral ischemia by reducing BBB leakage and minimizing edema in the brain tissue.

It has been demonstrated that cerebral IR injury initiates harmful processes in the brain, leading to oxidative stress and inflammation in brain tissue [68]. These changes are associated with BBB leakage, edema in the brain tissue, and behavioral impairments [33, 69]. Our findings illustrate that the induction of cerebral IR decreased the activities of antioxidant enzymes, such as SOD and glutathione peroxidase (GPX), while increasing the concentration of MDA in the hippocampal tissue. These results are consistent with previous studies that have investigated the effects of IR injury on oxidative stress markers in the hippocampus [70, 71]. Our findings demonstrate that treatment with rAD-MSC-CM and cLD-MSC-CM enhanced the activity of antioxidant enzymes, such as SOD and GPX, while decreasing MDA concentrations in the hippocampal tissue of rats subjected to IR. In line with these findings, other studies have shown that MSC-CM can prevent oxidative stress by restoring antioxidant enzyme levels [65, 72]. Oxidative stress has been associated with cognitive impairments and anxiety- or depression-like behaviors in rats [73, 74]. Thus, utilizing antioxidants may help alleviate these detrimental effects [75]. Furthermore, the antioxidant properties of MSC-CM have been reported in multiple studies [76]. MSC-CM is a heterogeneous substance that contains various soluble factors capable of decreasing lipid peroxidation while simultaneously enhancing the production of antioxidant enzymes [77, 78].

Pyramidal neurons in the CA1 region are particularly vulnerable to ischemic injury, leading to several pathological changes. These include shrinkage of the cell body, pyknosis (nuclear condensation), and a reduction in dendritic spines [11, 79]. Consistent with these studies, our findings indicated that the pyramidal cell bodies in the CA1 region of the hippocampus were shrunk and displayed pyknotic nuclei in the IR rats. These histopathological changes observed in the CA1 region may be attributed to increased BBB permeability, brain edema, and oxidative stress following ischemic stroke [11, 80, 81]. Our data indicated that the histopathological changes in the CA1 region were alleviated in rats treated with rAD-MSC-CM and cLD-MSC-CM. This improvement may be attributed to their antioxidative and neuroprotective properties of MSC-CM [82].

CONCLUSION

This study demonstrates that both rAD-MSC-CM and cLD-MSC-CM attenuate cerebral IR injury by reducing oxidative stress, preserving BBB integrity, and mitigating hippocampal damage. The comparable efficacy of these conditioned media suggests that their therapeutic benefits may arise from their antioxidant mechanisms rather than species-specific differences. These findings highlight the potential of MSC-CM as a cell-free therapeutic strategy for ischemic brain injury, warranting further investigation into standardized protocols for clinical translation.

AUTHORS' CONTRIBUTIONS

Maryam Khombi Shooshtari: Conceptualization, Writing - review & editing, Data curation. Sadegh Moradi Vastegani: Conceptualization, Writing - review & editing, Data curation. Yaghoob Farbood: Methodology, Writing - review & editing. Alireza Sarkaki: Methodology, Writing - review & editing. Vahid

Bayati: Investigation, Methodology. Fereshteh Nejaddehbashi: Investigation, Methodology. Seyed Esmaeil Khoshnam: Supervision, Conceptualization, Writing - review & editing, Visualization, Project administration, Funding acquisition, Formal analysis. Maryam Farzaneh: Supervision, Conceptualization, Writing - review & editing, Project administration. Maryam Khombi Shooshtari and Sadegh Moradi Vastegani, contributed equally to this manuscript

ETHICS APPROVAL AND CONSENT TO PARTICIPATE

All experimental procedures were permitted by the ethics committee at AJUMS, Ahvaz, Iran (Ethic code: IR.AJUMS.ABHC.REC.1400.075).

HUMAN AND ANIMAL RIGHTS

All experimental procedures followed NIH guidelines.

This study adheres to internationally accepted standards for animal research, following the 3Rs principle. The ARRIVE guidelines were employed for reporting experiments involving live animals, promoting ethical research practice.

CONSENT FOR PUBLICATION

Not applicable.

AVAILABILITY OF DATA AND MATERIALS

The data and supportive information are available within the article.

FUNDING

This article was financially supported by Ahvaz Jundishapur University of Medical Sciences, Ahvaz-Iran (Grant number: APRC-0015).

CONFLICT OF INTEREST

The authors declare no conflict of interest, financial or otherwise.

ACKNOWLEDGEMENTS

Declared none.

REFERENCES

[1] Feigin VL, Brainin M, Norrving B, *et al.* World Stroke Organization (WSO): Global stroke fact sheet 2022. Int J Stroke 2022; 17(1): 18-29. http://dx.doi.org/10.1177/17474930211065917 PMID: 34986727

[2] Farzaneh M, Anbiyaee O, Azizidoost S, *et al.* The mechanisms of long non-coding RNA-XIST in ischemic stroke: Insights into functional roles and therapeutic potential. Mol Neurobiol 2024; 61(5): 2745-53. http://dx.doi.org/10.1007/s12035-023-03740-x PMID: 37932544

[3] Dhapola R, Medhi B, HariKrishnaReddy D. Insight into the pathophysiological advances and molecular mechanisms underlying cerebral stroke: Current status. Mol Biol Rep 2024; 51(1): 649. http://dx.doi.org/10.1007/s11033-024-09597-0 PMID: 38733445

[4] Kuriakose D, Xiao Z. Pathophysiology and treatment of stroke: Present status and future perspectives. Int J Mol Sci 2020; 21(20): 7609. http://dx.doi.org/10.3390/ijms21207609 PMID: 33076218

[5] Zhang Y, Dong N, Hong H, Qi J, Zhang S, Wang J. Mesenchymal stem cells: Therapeutic mechanisms for stroke. Int J Mol Sci 2022; 23(5): 2550. http://dx.doi.org/10.3390/ijms23052550 PMID: 35269692

[6] Guo Y, Peng Y, Zeng H, Chen G. Progress in mesenchymal stem cell therapy for ischemic stroke. Stem Cells Int 2021; 2021(1): 1-24. http://dx.doi.org/10.1155/2021/9923566 PMID: 34221026

[7] El-Sayed ME, Atwa A, Sofy AR, *et al.* Mesenchymal stem cell transplantation in burn wound healing: Uncovering the mechanisms of local regeneration and tissue repair. Histochem Cell Biol 2024; 161(2): 165-81. http://dx.doi.org/10.1007/s00418-023-02244-y PMID: 37847258

[8] Giovannelli L, Bari E, Jommi C, *et al.* Mesenchymal stem cell secretome and extracellular vesicles for neurodegenerative diseases: Risk-benefit profile and next steps for the market access. Bioact Mater 2023; 29: 16-35. http://dx.doi.org/10.1016/j.bioactmat.2023.06.013 PMID: 37456581

[9] He J, Liu J, Huang Y, Tang X, Xiao H, Hu Z. Oxidative stress, inflammation, and autophagy: Potential targets of mesenchymal stem cells-based therapies in ischemic stroke. Front Neurosci 2021; 15: 641157. http://dx.doi.org/10.3389/fnins.2021.641157 PMID: 33716657

[10] Dhir N, Jain A, Sharma AR, *et al.* Rat BM-MSCs secretome alone and in combination with stiripentol and ISRIB, ameliorated microglial activation and apoptosis in experimental stroke. Behav Brain Res 2023; 449: 114471. http://dx.doi.org/10.1016/j.bbr.2023.114471 PMID: 37146724

[11] Einenkel AM, Salameh A. Selective vulnerability of hippocampal CA1 and CA3 pyramidal cells: What are possible pathomechanisms and should more attention be paid to the CA3 region in future studies? J Neurosci Res 2024; 102(1): e25276. http://dx.doi.org/10.1002/jnr.25276 PMID: 38284845

[12] Eslamizade MJ, Madjd Z, Rasoolijazi H, *et al.* Impaired memory and evidence of histopathology in CA1 pyramidal neurons through injection of Aβ1-42 peptides into the frontal cortices of rat. Basic Clin Neurosci 2016; 7(1): 31-41. PMID: 27303597

[13] Yaqubi S, Karimian M. Stem cell therapy as a promising approach for ischemic stroke treatment. Curr Res Pharmacol Drug Discov 2024; 6: 100183. http://dx.doi.org/10.1016/j.crphar.2024.100183 PMID: 38831867

[14] Raoufinia R, Rahimi HR, Saburi E, Moghbeli M. Advances and challenges of the cell-based therapies among diabetic patients. J Transl Med 2024; 22(1): 435. http://dx.doi.org/10.1186/s12967-024-05226-3 PMID: 38720379

[15] Taylor MR, Cole SW, Strom J, *et al.* Unfavorable transcriptome profiles and social disadvantage in hematopoietic cell transplantation: A CIBMTR analysis. Blood Adv 2023; 7(22): 6830-8. http://dx.doi.org/10.1182/bloodadvances.2023010746 PMID: 37773924

[16] Rahimi B, Panahi M, Saraygord-Afshari N, *et al.* The secretome of mesenchymal stem cells and oxidative stress: Challenges and opportunities in cell-free regenerative medicine. Mol Biol Rep 2021; 48(7): 5607-19. http://dx.doi.org/10.1007/s11033-021-06360-7 PMID: 34191238

[17] Karimian A, Khoshnazar SM, Kazemi T, Asadi A, Abdolmaleki A. Role of secretomes in cell-free therapeutic strategies in regenerative medicine. Cell Tiss Bank 2023; 25(2): 1-16.

http://dx.doi.org/10.1007/s10561-023-10073-5 PMID: 36725732

[18] Castelli V, Antonucci I, d'Angelo M, *et al.* Neuroprotective effects of human amniotic fluid stem cells-derived secretome in an ischemia/reperfusion model. Stem Cells Transl Med 2021; 10(2): 251-66. http://dx.doi.org/10.1002/sctm.20-0268 PMID: 33027557

[19] Seo HG, Yi Y, Oh BM, Paik NJ. Neuroprotective effect of secreted factors from human adipose stem cells in a rat stroke model. Neurol Res 2017; 39(12): 1114-24. http://dx.doi.org/10.1080/01616412.2017.1379293 PMID: 28948857

[20] Jiang RH, Wu CJ, Xu XQ, *et al.* Hypoxic conditioned medium derived from bone marrow mesenchymal stromal cells protects against ischemic stroke in rats. J Cell Physiol 2019; 234(2): 1354-68. http://dx.doi.org/10.1002/jcp.26931 PMID: 30076722

[21] Zhang Y, Ma L, Su Y, *et al.* Hypoxia conditioning enhances neuroprotective effects of aged human bone marrow mesenchymal stem cell-derived conditioned medium against cerebral ischemia *in vitro*. Brain Res 2019; 1725: 146432. http://dx.doi.org/10.1016/j.brainres.2019.146432 PMID: 31491422

[22] Liu G, Wang D, Jia J, *et al.* Neuroprotection of human umbilical cord-derived mesenchymal stem cells (hUC-MSCs) in alleviating ischemic stroke-induced brain injury by regulating inflammation and oxidative stress. Neurochem Res 2024; 49(10): 2871-87. http://dx.doi.org/10.1007/s11064-024-04212-x PMID: 39026086

[23] Choudhery MS, Arif T, Mahmood R, Harris DT. Stem cell-based acellular therapy: Insight into biogenesis, bioengineering and therapeutic applications of exosomes. Biomolecules 2024; 14(7): 792. http://dx.doi.org/10.3390/biom14070792 PMID: 39062506

[24] Wang Y, Yi H, Song Y. The safety of MSC therapy over the past 15 years: A meta-analysis. Stem Cell Res Ther 2021; 12(1): 545. http://dx.doi.org/10.1186/s13287-021-02609-x PMID: 34663461

[25] Jeon D, Chu K, Lee ST, *et al.* Neuroprotective effect of a cell-free extract derived from human adipose stem cells in experimental stroke models. Neurobiol Dis 2013; 54: 414-20. http://dx.doi.org/10.1016/j.nbd.2013.01.015 PMID: 23376682

[26] Tang L, Xu Y, Wang L, Pan J. Adipose-derived stem cell exosomes ameliorate traumatic brain injury through the NLRP3 signaling pathway. Neuroreport 2023; 34(13): 677-84. http://dx.doi.org/10.1097/WNR.0000000000001941 PMID: 37506308

[27] Amini N, Nejaddehbashi F, Badavi M, Bayati V, Zahra Basir . Combined effect of naringin and adipose tissue-derived mesenchymal stem cell on cisplatin nephrotoxicity through Sirtuin1/Nrf-2/HO-1 signaling pathway: A promising nephroprotective candidate. Cell Tissue Res 2024; 397(3): 193-204. http://dx.doi.org/10.1007/s00441-024-03902-w PMID: 38953985

[28] Mahdavi R, Akbari Jonoush Z, Ghafourian M, Khoshnam SE, Nezhad Dehbashi F, Farzaneh M. The effect of remdesivir as an anti-COVID-19 drug on chicken hepatocyte enzymes: An *in vitro* study. Iran J Med Microbiol 2023; 17(3): 309-17. http://dx.doi.org/10.30699/ijmm.17.3.309

[29] Akbari Jonoush Z, Mahdavi R, Ghafourian M, Khoshnam SE, Nezhad Dehbashi F, Farzaneh M. The effect of remdesivir as an anti-COVID-19 drug on the secretion of inflammatory markers by chicken liver cells: An *in vitro* study. J Inflammat Dis 2023; 26(4): 173-82. http://dx.doi.org/10.32598/JID.26.4.2

[30] Sun HS, Jackson MF, Martin LJ, *et al.* Suppression of hippocampal TRPM7 protein prevents delayed neuronal death in brain ischemia. Nat Neurosci 2009; 12(10): 1300-7. http://dx.doi.org/10.1038/nn.2395 PMID: 19734892

[31] Vastegani SM, Hajipour S, Sarkaki A, *et al.* Curcumin ameliorates neurobehavioral deficits in ambient dusty particulate matter-exposure rats: The role of oxidative stress. Neurochem Res 2023; 48(6): 1798-810. http://dx.doi.org/10.1007/s11064-023-03877-0 PMID: 36708454

[32] Belayev L, Busto R, Ikeda M, *et al.* Protection against blood–brain barrier disruption in focal cerebral ischemia by the type IV phosphodiesterase inhibitor BBB022: A quantitative study. Brain Res 1998; 787(2): 277-85. http://dx.doi.org/10.1016/S0006-8993(97)01499-6 PMID: 9518648

[33] Khoshnam SE, Farbood Y, Fathi Moghaddam H, Sarkaki A, Badavi M, Khorsandi L. Vanillic acid attenuates cerebral hyperemia, blood-brain barrier disruption and anxiety-like behaviors in rats following transient bilateral common carotid occlusion and reperfusion. Metab Brain Dis 2018; 33(3): 785-93. http://dx.doi.org/10.1007/s11011-018-0187-5 PMID: 29356980

[34] Gerriets T, Walberer M, Ritschel N, *et al.* Edema formation in the hyperacute phase of ischemic stroke. J Neurosurg 2009; 111(5): 1036-42. http://dx.doi.org/10.3171/2009.3.JNS081040 PMID: 19408985

[35] Xiao W, Shi J. Application of adipose-derived stem cells in ischemic heart disease: Theory, potency, and advantage. Front Cardiovasc Med 2024; 11: 1324447. http://dx.doi.org/10.3389/fcvm.2024.1324447 PMID: 38312236

[36] Kostecka A, Kalamon N, Skoniecka A, *et al.* Adipose-derived mesenchymal stromal cells in clinical trials: Insights from single-cell studies. Life Sci 2024; 351: 122761. http://dx.doi.org/10.1016/j.lfs.2024.122761 PMID: 38866216

[37] Bunnell BA. Adipose tissue-derived mesenchymal stem cells. Cells 2021; 10(12): 3433. http://dx.doi.org/10.3390/cells10123433

[38] Moll G, Alm JJ, Davies LC, *et al.* Do cryopreserved mesenchymal stromal cells display impaired immunomodulatory and therapeutic properties? Stem Cells 2014; 32(9): 2430-42. http://dx.doi.org/10.1002/stem.1729 PMID: 24805247

[39] Levy O, Kuai R, Siren EMJ, *et al.* Shattering barriers toward clinically meaningful MSC therapies. Sci Adv 2020; 6(30): eaba6884. http://dx.doi.org/10.1126/sciadv.aba6884 PMID: 32832666

[40] Sadr S, Lotfalizadeh N, Ghaniei A, Ahmadi Simab P, Hajjafari A. An update on characterisation and applications of mesenchymal stem cells from chickens with challenges and prospective review. Worlds Poult Sci J 2024; 80(2): 589-610. http://dx.doi.org/10.1080/00439339.2023.2288321

[41] Maryam F, Shirin A. *In vitro* generation of hepatocytes across different stages of chicken embryos. Curr Mol Med 2024; 1: 843. http://dx.doi.org/10.21203/rs.3.rs-4095843/v1

[42] Panta A, Montgomery K, Nicolas M, Mani KK, Sampath D, Sohrabji F. Mir363-3p treatment attenuates long-term cognitive deficits precipitated by an ischemic stroke in middle-aged female rats. Front Aging Neurosci 2020; 12: 586362. http://dx.doi.org/10.3389/fnagi.2020.586362 PMID: 33132904

[43] Ögren S, Stiedl O. Passive avoidance. Amsterdam, Netherlands: Elsevier 2010; pp. 1-6.

[44] D'Souza CE, Greenway MRF, Graff-Radford J, Meschia JF. Cognitive impairment in patients with stroke. Semin Neurol 2021; 40: 75-84. http://dx.doi.org/10.1055/s-0040-1722217 PMID: 33418591

[45] Lee SS, Kim CJ, Shin MS, Lim BV. Treadmill exercise ameliorates memory impairment through ERK-Akt-CREB-BDNF signaling pathway in cerebral ischemia gerbils. J Exerc Rehabil 2020; 16(1): 49-57. http://dx.doi.org/10.12965/jer.2040014.007 PMID: 32161734

[46] Kirino T. Delayed neuronal death. Neuropathology 2000; 20(s1)(Suppl.): 95-7. http://dx.doi.org/10.1046/j.1440-1789.2000.00306.x PMID: 11037198

[47] Zhou LYY, Wright TE, Clarkson AN. Prefrontal cortex stroke induces delayed impairment in spatial memory. Behav Brain Res 2016; 296: 373-8. http://dx.doi.org/10.1016/j.bbr.2015.08.022 PMID: 26306825

[48] Cauda F, Nani A, Manuello J, *et al.* Brain structural alterations are distributed following functional, anatomic and genetic connectivity. Brain 2018; 141(11): 3211-32. http://dx.doi.org/10.1093/brain/awy252 PMID: 30346490

[49] Wang W, Redecker C, Bidmon HJ, Witte OW. Delayed neuronal death and damage of GDNF family receptors in CA1 following focal cerebral ischemia. Brain Res 2004; 1023(1): 92-101. http://dx.doi.org/10.1016/j.brainres.2004.07.034 PMID: 15364023

[50] Cunningham CJ, Redondo-Castro E, Allan SM. The therapeutic potential of the mesenchymal stem cell secretome in ischaemic stroke. J Cereb Blood Flow Metab 2018; 38(8): 1276-92. http://dx.doi.org/10.1177/0271678X18776802 PMID: 29768965

[51] Drago D, Cossetti C, Iraci N, *et al.* The stem cell secretome and its role in brain repair. Biochimie 2013; 95(12): 2271-85. http://dx.doi.org/10.1016/j.biochi.2013.06.020 PMID: 23827856

[52] Bagheri-Mohammadi S. Protective effects of mesenchymal stem cells on ischemic brain injury: Therapeutic perspectives of regenerative medicine. Cell Tissue Bank 2021; 22(2): 249-62. http://dx.doi.org/10.1007/s10561-020-09885-6 PMID: 33231840

[53] Asgari Taei A, Dargahi L, Nasoohi S, Hassanzadeh G, Kadivar M, Farahmandfar M. The conditioned medium of human embryonic stem cell-derived mesenchymal stem cells alleviates neurological deficits and improves synaptic recovery in experimental stroke. J Cell Physiol 2021; 236(3): 1967-79. http://dx.doi.org/10.1002/jcp.29981 PMID: 32730642

[54] Vicentini JE, Weiler M, Almeida SRM, de Campos BM, Valler L, Li LM. Depression and anxiety symptoms are associated to disruption of default mode network in subacute ischemic stroke. Brain Imaging Behav 2017; 11(6): 1571-80. http://dx.doi.org/10.1007/s11682-016-9605-7 PMID: 27743373

[55] Redmond C, Bushnell C, Duncan P, *et al.* Association of in-hospital depression and anxiety symptoms following stroke with 3 months- depression, anxiety and functional outcome. J Clin Neurosci 2022; 98: 133-6. http://dx.doi.org/10.1016/j.jocn.2022.02.010 PMID: 35180502

[56] Scharf AC, Gronewold J, Eilers A, *et al.* Depression and anxiety in acute ischemic stroke involving the anterior but not paramedian or inferolateral thalamus. Front Psychol 2023; 14: 1218526. http://dx.doi.org/10.3389/fpsyg.2023.1218526 PMID: 37701875

[57] Ignacio KHD, Muir RT, Diestro JDB, *et al.* Prevalence of depression and anxiety symptoms after stroke in young adults: A systematic review and meta-analysis. J Stroke Cerebrovasc Dis 2024; 33(7): 107732. http://dx.doi.org/10.1016/j.jstrokecerebrovasdis.2024.107732 PMID: 38657829

[58] Ranjbaran M, Kianian F, Kadkhodaee M, *et al.* Mesenchymal stem cells and their conditioned medium as potential therapeutic strategies in managing comorbid anxiety in rat sepsis induced by cecal ligation and puncture. Iran J Basic Med Sci 2022; 25(6): 690-7. PMID: 35949300

[59] Kraeuter A-K, Guest PC, Sarnyai Z. The open field test for measuring locomotor activity and anxiety-like behavior. Meth Mol Biol 2019; 1916: 99-103. http://dx.doi.org/10.1007/978-1-4939-8994-2_9 PMID: 30535687

[60] Balkaya M, Kröber JM, Rex A, Endres M. Assessing post-stroke behavior in mouse models of focal ischemia. J Cereb Blood Flow Metab 2013; 33(3): 330-8. http://dx.doi.org/10.1038/jcbfm.2012.185 PMID: 23232947

[61] Cunningham CJ, Wong R, Barrington J, Tamburrano S, Pinteaux E, Allan SM. Systemic conditioned medium treatment from interleukin-1 primed mesenchymal stem cells promotes recovery after stroke. Stem Cell Res Ther 2020; 11(1): 32. http://dx.doi.org/10.1186/s13287-020-1560-y PMID: 31964413

[62] Ozkan S, Isildar B, Sahin H, Saygi HI, Konukoglu D, Koyuturk M. Comparative analysis of effects of conditioned mediums obtained from 2D or 3D cultured mesenchymal stem cells on kidney functions of diabetic rats: Early intervention could potentiate transdifferentiation of parietal epithelial cell into podocyte precursors. Life Sci 2024; 343: 122543. http://dx.doi.org/10.1016/j.lfs.2024.122543 PMID: 38460812

[63] Mirshekari Jahangiri H, Sarkaki A, Farbood Y, Dianat M, Goudarzi G. Gallic acid affects blood-brain barrier permeability, behaviors, hippocampus local EEG, and brain oxidative stress in ischemic rats exposed to dusty particulate matter. Environ Sci Pollut Res Int 2020; 27(5): 5281-92. http://dx.doi.org/10.1007/s11356-019-07076-9 PMID: 31848951

[64] Blanchette M, Daneman R. Formation and maintenance of the BBB. Mech Dev 2015; 138(Pt 1): 8-16. http://dx.doi.org/10.1016/j.mod.2015.07.007 PMID: 26215350

[65] Saleem R, Mohamed-Ahmed S, Elnour R, Berggreen E, Mustafa K, Al-Sharabi N. Conditioned Medium from Bone Marrow Mesenchymal Stem Cells Restored Oxidative Stress-Related Impaired Osteogenic Differentiation. Int J Mol Sci 2021; 22(24): 13458. http://dx.doi.org/10.3390/ijms222413458 PMID: 34948255

[66] Fatemi I, Saeed-Askari P, Hakimizadeh E, *et al.* Long-term metformin therapy improves neurobehavioral functions and antioxidative activity after cerebral ischemia/reperfusion injury in rats. Brain Res Bull 2020; 163: 65-71. http://dx.doi.org/10.1016/j.brainresbull.2020.07.015 PMID: 32693150

[67] Chen Y, Garcia GE, Huang W, Constantini S. The involvement of secondary neuronal damage in the development of neuropsychiatric disorders following brain insults. Front Neurol 2014; 5: 22. http://dx.doi.org/10.3389/fneur.2014.00022 PMID: 24653712

[68] Khoshnam SE, Winlow W, Farzaneh M, Farbood Y, Moghaddam HF. Pathogenic mechanisms following ischemic stroke. Neurol Sci 2017; 38(7): 1167-86. http://dx.doi.org/10.1007/s10072-017-2938-1 PMID: 28417216

[69] Shushanyan RA, Avtandilyan NV, Grigoryan AV, Karapetyan AF. The role of oxidative stress and neuroinflammatory mediators in the pathogenesis of high-altitude cerebral edema in rats. Respir Physiol Neurobiol 2024; 327: 104286. http://dx.doi.org/10.1016/j.resp.2024.104286 PMID: 38825093

[70] Shang J, Jiao J, Yan M, *et al.* Chrysin protects against cerebral ischemia-reperfusion injury in hippocampus *via* restraining oxidative stress and transition elements. Biomed Pharmacother 2023; 161: 114534. http://dx.doi.org/10.1016/j.biopha.2023.114534 PMID: 36933376

[71] Liu D, Wang H, Zhang Y, Zhang Z. Protective effects of chlorogenic acid on cerebral ischemia/reperfusion injury rats by regulating oxidative stress-related Nrf2 pathway. Drug Des Devel Ther 2020; 14: 51-60. http://dx.doi.org/10.2147/DDDT.S228751 PMID: 32021091

[72] Hong HE, Kim OH, Kwak BJ, *et al.* Antioxidant action of hypoxic conditioned media from adipose-derived stem cells in the hepatic injury of expressing higher reactive oxygen species. Ann Surg Treat Res 2019; 97(4): 159-67. http://dx.doi.org/10.4174/astr.2019.97.4.159 PMID: 31620389

[73] Hosseini M, Baghcheghi Y, Salmani H, Beheshti F. Contribution of brain tissue oxidative damage in hypothyroidism-associated learning and memory impairments. Adv Biomed Res 2017; 6(1): 59.

http://dx.doi.org/10.4103/2277-9175.206699 PMID: 28584813

[74] Patki G, Solanki N, Atrooz F, Allam F, Salim S. Depression, anxiety-like behavior and memory impairment are associated with increased oxidative stress and inflammation in a rat model of social stress. Brain Res 2013; 1539: 73-86. http://dx.doi.org/10.1016/j.brainres.2013.09.033 PMID: 24096214

[75] Albaqami FF, Abdel-Rahman RF, Althurwi HN, *et al.* Targeting inflammation and oxidative stress for protection against ischemic brain injury in rats using cupressuflavone. Saudi Pharm J 2024; 32(1): 101933. http://dx.doi.org/10.1016/j.jsps.2023.101933 PMID: 38204594

[76] Wang Y, Liu J, Yu B, *et al.* Umbilical cord-derived mesenchymal stem cell conditioned medium reverses neuronal oxidative injury by inhibition of TRPM2 activation and the JNK signaling pathway. Mol Biol Rep 2022; 49(8): 7337-45. http://dx.doi.org/10.1007/s11033-022-07524-9 PMID: 35585377

[77] Ma N, Li S, Lin C, Cheng X, Meng Z. Mesenchymal stem cell conditioned medium attenuates oxidative stress injury in hepatocytes partly by regulating the miR-486-5p/PIM1 axis and the TGF-β/Smad pathway. Bioengineered 2021; 12(1): 6434-47. http://dx.doi.org/10.1080/21655979.2021.1972196 PMID: 34519263

[78] Park CM, Kim MJ, Kim SM, Park JH, Kim ZH, Choi YS. Umbilical cord mesenchymal stem cell-conditioned media prevent muscle atrophy by suppressing muscle atrophy-related proteins and ROS generation. In Vitro Cell Dev Biol Anim 2016; 52(1): 68-76. http://dx.doi.org/10.1007/s11626-015-9948-1 PMID: 26373864

[79] Merino-Serrais P, Plaza-Alonso S, Hellal F, *et al.* Structural changes of CA1 pyramidal neurons after stroke in the contralesional hippocampus. Brain Pathol 2024; 34(3): e13222. http://dx.doi.org/10.1111/bpa.13222 PMID: 38012061

[80] Colbourne F, Li H, Buchan AM, Clemens JA. Continuing postischemic neuronal death in CA1: Influence of ischemia duration and cytoprotective doses of NBQX and SNX-111 in rats. Stroke 1999; 30(3): 662-8. http://dx.doi.org/10.1161/01.STR.30.3.662 PMID: 10066868

[81] Yamaguchi S, Ogata H, Hamaguchi S, Kitajima T. Superoxide radical generation and histopathological changes in hippocampal CA1 after ischaemia/ reperfusion in gerbils. Can J Anaesth 1998; 45(3): 226-32. http://dx.doi.org/10.1007/BF03012907 PMID: 9579260

[82] Huang Y, Mei X, Jiang W, *et al.* Mesenchymal stem cell-conditioned medium protects hippocampal neurons from radiation damage by suppressing oxidative stress and apoptosis. Dose Resp 2021; 19(1): 1559325820984944. http://dx.doi.org/10.1177/1559325820984944 PMID: 33716588